Comprehensive analysis of long non-coding RNA s and mRNAs in skeletal muscle of diabetic Goto-Kakizaki rats during the early stage of type 2 diabetes

Wenlu Zhang [1], **Yunmeng Bai** [1], **Zixi Chen** [1], **Xingsong Li** [1], **Shuying Fu** [1], **Lizhen Huang** [1], **Shudai Lin** [Corresp., 1], **Hongli Du** [Corresp. 1]

[1] School of Biology and Biological Engineering, South China University of Technology, Guangzhou, China

Corresponding Authors: Shudai Lin, Hongli Du
Email address: linsd@scut.edu.cn, hldu@scut.edu.cn

Skeletal muscle long non-coding RNAs (lncRNAs) were reported to be involved in the development of type 2 diabetes (T2D). However, little is known about the mechanism of skeletal muscle lncRNAs on hyperglycemia of diabetic Goto-Kakizaki (GK) rats at the age of 3 and 4 weeks. To elucidate this, we used RNA-sequencing to profile the skeletal muscle transcriptomes including lncRNAs and mRNAs, in diabetic GK and control Wistar rats at the age of 3 and 4 weeks. Totally, there were 438 differentially expressed mRNAs (DEGs) and 401 differentially expressed lncRNAs (DELs) in skeletal muscle of 3-week-old GK rats compared with age-matched Wistar rats, and 1000 DEGs and 726 DELs between GK rats and Wistar rats at 4 weeks of age. The protein-protein interaction analysis of overlapping DEGs between 3 and 4 weeks, the correlation analysis of DELs and DEGs, as well as the prediction of target DEGs of DELs showed that these DEGs (*Pdk4*, *Stc2*, *Il15*, *Fbxw7* and *Ucp3*) might play key roles in hyperglycemia, glucose intolerance, and increased fatty acid oxidation. Considering the corresponding co-expressed DELs with high correlation coefficients or targeted DELs of these DEGs, our study indicated that these dysregulated lncRNA-mRNA pairs (NONRATG017315.2-*Pdk4*, NONRATG003318.2-*Stc2*, NONRATG011882.2-*Il15*, NONRATG013497.2-*Fbxw7*, MSTRG.1662-*Ucp3*) might be related to above biological processes in GK rats at the age of 3 and 4 weeks. Our study could provide more comprehensive knowledge of mRNAs and lncRNAs in skeletal muscle of GK rats at 3 and 4 weeks of age. And our study may provide deeper understanding of the underlying mechanism in T2D of GK rats at the age of 3 and 4 weeks.

Comprehensive analysis of long non-coding RNAs and mRNAs in skeletal muscle of diabetic Goto-Kakizaki rats during the early stage of type 2 diabetes

Wenlu Zhang, Yunmeng Bai, Zixi Chen, Xingsong Li, Shuying Fu, Lizhen Huang, Shudai Lin* and Hongli Du*

School of Biology and Biological Engineering, South China University of Technology, Guangzhou, Guangdong, China.

***Corresponding authors**:

Hongli Du, hldu@scut.edu.cn

Shudai Lin, linsd@scut.edu.cn

School of Biology and Biological Engineering, South China University of Technology, 382 Zhonghuan Road East, Panyu District, Guangzhou Higher Education Mega Centre, Guangzhou 510006, Guangdong, China

Abstract

Skeletal muscle long non-coding RNAs (lncRNAs) were reported to be involved in the development of type 2 diabetes (T2D). However, little is known about the mechanism of skeletal muscle lncRNAs on hyperglycemia of diabetic Goto-Kakizaki (GK) rats at the age of 3 and 4 weeks. To elucidate this, we used RNA-sequencing to profile the skeletal muscle transcriptomes including lncRNAs and mRNAs, in diabetic GK and control Wistar rats at the age of 3 and 4 weeks. Totally, there were 438 differentially expressed mRNAs (DEGs) and 401 differentially expressed lncRNAs (DELs) in skeletal muscle of 3-week-old GK rats compared with age-matched Wistar rats, and 1000 DEGs and 726 DELs between GK rats and Wistar rats at 4 weeks of age. The protein-protein interaction analysis of overlapping DEGs between 3 and 4 weeks, the correlation analysis of DELs and DEGs, as well as the prediction of target DEGs of DELs showed that these DEGs (*Pdk4*, *Stc2*, *Il15*, *Fbxw7* and *Ucp3*) might play key roles in hyperglycemia, glucose intolerance, and increased fatty acid oxidation. Considering the corresponding co-expressed DELs with high correlation coefficients or targeted DELs of these DEGs, our study indicated that these dysregulated lncRNA-mRNA pairs (NONRATG017315.2-*Pdk4*, NONRATG003318.2-*Stc2*, NONRATG011882.2-*Il15*, NONRATG013497.2-*Fbxw7*, MSTRG.1662-*Ucp3*) might be related to above biological processes in GK rats at the age of 3 and 4 weeks. Our study could provide more comprehensive knowledge of mRNAs and lncRNAs in skeletal muscle of GK rats at 3 and 4 weeks of age. And our study may provide deeper understanding of the underlying mechanism in T2D of GK rats at the age of 3 and 4 weeks.

Introduction

It has been demonstrated that approximately 75% human genome is transcribed, and nearly 97% genomic DNA cannot be translated into proteins (Djebali et al. 2012). These RNAs without protein-coding ability are known as non-coding RNAs (ncRNAs). Among them, long ncRNAs (lncRNAs) are more than 200 nucleotides in length (Esteller 2011; Guttman & Rinn 2012), exhibiting tissue-specific (Cabili et al. 2011; Mercer et al. 2008; Tsoi et al. 2015) and low

expression levels (Derrien et al. 2012). They could promote (Guil & Esteller 2012; Luo & Chen 2016) or suppress (Espinoza et al. 2004; Peterlin et al. 2012; Rinn et al. 2007) the expression level of their target genes. Furthermore, it has been revealed that the expression of lncRNAs was dysregulated in many diseases, such as type 2 diabetes (T2D) (Akerman et al. 2017; Liu et al. 2014; Reddy et al. 2014).

As it was uncovered, lncRNAs were closely correlated to T2D. Upregulated expression of lncRNA Meg3 could contribute to insulin resistance in *ob/ob* mice liver (Zhu et al. 2016). The *db/db* mice islets showed significantly decreased expression of lncRNA Meg3, and the islet-specific knockdown of lncRNA Meg3 resulted in less insulin synthesis and secretion but larger scale of β cell apoptosis, consequently lead to impaired glucose tolerance (You et al. 2016). The islet-specific lncRNA Tug1 knockdown mice exhibited an increased apoptosis ratio and a lower insulin secretion in the β cells (Yin et al. 2015; You et al. 2016). Besides, the reduced expression of lncRNA H19 could impair insulin sensitivity and decrease glucose uptake in muscle cells (Gao et al. 2014). Moreover, significantly decreased expression of H19 was observed in muscle of T2D patients (Gao et al. 2014), suggesting the importance of skeletal muscle lncRNAs to the development of T2D. As one of the target tissues of insulin, skeletal muscle is burdened with 70%-80% postprandial glucose disposal responsibility (Baron et al. 1988; DeFronzo et al. 1981). Therefore, lncRNAs in skeletal muscle might play critical roles in regulating whole-body glucose homeostasis and T2D development.

As a non-obese model for T2D, Goto-Kakizaki (GK) rats are produced by selective breeding from Wistar rats with impaired glucose tolerance (Goto et al. 1976; Kitahara et al. 1978). GK rats show postprandial glucose intolerance and insulin resistance in skeletal muscle and adipose tissue (Bisbis et al. 1993; Portha et al. 2012), and exhibit hyperglycemia during age of 3-4 weeks (Ando et al. 2018). Though GK rats has been found to exhibit defects in skeletal muscle and their related mRNA expression level has been investigated (Dadke et al. 2000; Steiler et al. 2003), the regulation mechanism of skeletal muscle lncRNA to postprandial hyperglycemia in GK rat at the age of 3 and 4 weeks is still indistinct.

To explore the role of skeletal muscle lncRNAs in hyperglycemia development, we compared the skeletal muscle transcriptomes between T2D GK rats and control Wistar rats, to find out the differentially expressed mRNAs (DEGs) and differentially expressed lncRNAs (DELs). Subsequently, we conducted protein-protein interaction analysis, screened the co-expressed lncRNA-mRNA pairs with high correlation coefficients, and predicted the target mRNAs of DELs and the target microRNAs (miRNAs) of key DEGs and DELs. Our results suggested that the dysregulated lncRNAs might be implicated in hyperglycemia, glucose intolerance, as well as dysregulated glucose and fatty acid oxidation in skeletal muscle of GK rats at the age of 3 and 4 weeks. These findings might help us understand more about the regulation mechanism of skeletal muscle lncRNAs in T2D development.

Materials and methods

Ethical approval

The study was approved by the institutional review board of the Guangdong Key Laboratory of Laboratory Animals. All protocols were carried out in accordance with the guidelines of the Institutional Animal Care and Use Committee (IACUC) [Ethics certificate No.: IACUC2014029].

Animal breeding and tissues samples collection

Four groups of rats (diabetic male GK rats and control male Wistar rats at 3 weeks of age, diabetic male GK rats and diabetic male GK rats at 4 weeks of age, n = 10 each group), totally 40 subjects were used in this study. Rats were raised in a room with 12 hours dark: 12 hours light cycle, 20 to 25°C temperature and 60 ± 5% humidity, at the SLAC Laboratory Animal Co., Ltd. (Shanghai, China) (Almon et al. 2012; Nie et al. 2017; Nie et al. 2011; Xue et al. 2011). All animals were free access to food and water. Body weight of each rat was measured weekly by weighing. Food disappearance was measured by weighing the difference in the weight of feed added and the feed remaining. The behavior of rats including feeding, drinking, sleeping and

digging were observed. Blood samples were collected from the orbital plexus veins behind the eyeball using EDTA (4 mM final concentration) as an anticoagulant. Plasma was obtained from blood after centrifugation (2000 ×g, 4℃, 15 min), divided into aliquots, and then stored at −80℃. All rats were administered anesthesia with pentobarbital sodium (intraperitoneal, 50 mg/kg body weight), then were killed by cervical dislocation. Samples of gastrocnemius muscle of each rats were harvested, followed by rapidly frozen in liquid nitrogen, and stored at −80℃ for future studies (Nie et al. 2017; Nie et al. 2011). Six gastrocnemius muscle samples from six rats each group were selected randomly for RNA-sequencing in the present study.

Measurement of plasma glucose and insulin concentration

The automatic Dry Biochemical Analyzer FUJIFILM DRI-CHEM 7000i with GLU-PIII slides (Fujifilm, Saitama, Japan) was used to measure random plasma glucose concentration. And Thermo scientific Rat Insulin ELISA Kit (Cat#ERINS, Invitrogen, Waltham, MA, USA) was used to measured plasma insulin concentration. Assays were conducted according to the manufacturer's instructions.

RNA extraction and sequencing

Total RNA for RNA-sequencing was extracted from red part of each gastrocnemius muscle using TRIzol Reagent (Cat#15596-018, Life Technologies, Carlsbad, CA, USA) following the manufacturer's instructions. RNA integrity and concentration were measured by the Bioanalyzer 2100 system (Agilent Technologies, Santa Clara, CA, USA). Ribosomal RNA was removed using Epicentre Ribo-Zero™ Gold Kits (Epicentre, Madison, WI, USA) according to the manufacturer's instructions. RNA-sequencing was performed on Illumina HiSeq X Ten system (Illumina) following the HiSeq X Ten User Guide to generate 150 bp paired-end reads.

Analysis of differentially expressed mRNAs and lncRNAs

After quality control and filtering of low quality reads, we used STAR (Dobin & Gingeras 2015) version 020201 to align the cleaned reads of each sample to the Rattus norvegicus reference genome (Ensembl Rnor_6.0 version 92) with the parameters of --quantMode GeneCounts --outSAMstrandField intronMotif --outSAMtype BAM SortedByCoordinate --outSAMtype BAM SortedByCoordinate --twopassMode Basic. All the corresponding annotation files of Rattus_norvegicus.Rnor_6.0.92.gtf (ftp://ftp.ensembl.org/pub/release-92/gtf/rattus_norvegicus) and NONCODEv5_rat_rn6_lncRNA.gtf were downloaded from the Ensembl database54 and NONCODE version v5.0 (http://www.noncode.org/datadownload/NONCODEv5_rat_rn6_lncRNA.gtf.gz), respectively. Cufflinks were used for alignment of novel transcripts. Then the coding-probability of novel transcripts were identified by CPC2 (Kang et al. 2017), CPAT (Wang et al. 2013b) and CNCI (Sun et al. 2013). The novel transcripts with low coding-probability, or without coding-probability should meet the criteria: coding_probability score less than 0.5 in CPC2 and CPAT, and identified as noncoding by CNCI. Those novel transcripts meet criteria above with ≥ 200 bp in length and at least two exons, were defined as novel lncRNAs. Stringtie (Pertea et al. 2015) version 1.3.0 was used to assemble novel lncRNAs, annotated lncRNAs and annotated mRNAs transcripts. The novel lncRNAs were shown in Table S1. Ballgown R package (Frazee et al. 2015) version 2.10.0 was used to estimate the fragments per kilobase of exon per million fragments mapped (FPKM) of lncRNAs and mRNAs. The lncRNAs and mRNAs were filtered with FPKM < 0.5 (Moran et al. 2012). The FPKM from four groups of rats correspond to normal distribution based on the shapiro.test of Shapiro–Wilk test. The normal distribution of FPKM of four groups of rats were shown in Table S2. Next, the FPKM of GK rats at the age of 3 weeks were compared to Wistar rats at the age of 3 weeks, and GK rats at the age of 4 weeks were compared to Wistar rats at the age of 4 weeks. Thus, the differentially expressed lncRNAs (DELs) and differentially expressed mRNAs (DEGs) were obtained by Bayes-regularized t-test with an false discovery rate (FDR) correction using Cyber-T bayesreg (Kayala & Baldi 2012).

144 FDR < 0.05 was regarded as statistically significant. The power of test was calculated by
145 pwr.t.test in R package pwr. The flowchart of data analysis was shown in Fig. 1.

146 *Analysis of KEGG pathways and GO*

147 A Database for Annotation, Visualization and Integrated Discovery (DAVID) version 6.8
148 was used to obtain the Kyoto Encyclopedia of Genes and Genomes (KEGG) pathways and
149 biological process in Gene Ontology (GO). The statistical significance threshold was $P < 0.05$.

150 *Protein-protein interaction*

151 An online database resource Search Tool for the Retrieval of Interacting Genes (STRING)
152 (Szklarczyk et al. 2011) version 11.0 was performed to analyze protein-protein interaction of
153 overlapping upregulated mRNAs and downregulated mRNAs between 3 and 4 weeks,
154 respectively. After filtering disconnected nodes, we selected the minimum confidence score
155 above 0.4 of the interaction. The confidence score was a combined score of neighborhood on
156 chromosome, gene fusion, phylogenetic cooccurrence, homology, co-expression, experimentally
157 determined interaction, database annotated, and automated text-mining. Those connected nodes
158 with confidence score were downloaded for constructing the networks of protein-protein
159 interaction.

160 *The correlation analysis of lncRNAs and mRNAs*

161 Python version 3.6.4 was conducted to calculate the Pearson correlation coefficients of
162 lncRNAs and mRNAs. Those selected co-expressed lncRNA-mRNA pairs met the following
163 criteria: correlation coefficient value > 0.9, and the absolute fold change of these DEGs and
164 DELs ≥ 1.5. Then, pwr.r.test in R package pwr was carried out to calculate the power of the
165 correlation.

166 *Prediction of target genes of DELs*

167 Since over 65% of lncRNAs were located within 10 kb of genes (Jia et al. 2010), we
168 utilized the University of California Santa Cruz (UCSC) genome browser to identify potential
169 cis-target genes located within 10 kb of lncRNAs (Liang et al. 2017). Then the Basic Local
170 Alignment Search Tool (BLAST) was applied to screen mRNAs that have complementary
171 sequences to lncRNAs, followed by RNAplex (Liang et al. 2017) to identify trans-regulated
172 target genes of lncRNAs. Subsequently, DELs and their corresponding target DEGs were
173 obtained.

174 *Prediction of microRNAs both targeted to key DELs and DEGs*

175 We predicted the target microRNAs (miRNAs) of DELs and DEGs in key lncRNA-mRNA
176 pairs. TargetScan (Agarwal et al. 2015) was carried out to predict the target miRNAs of key
177 DEGs, and the RNAhybrid (Rehmsmeier et al. 2004) was applied to predict the target miRNAs
178 of key DELs.

179 *Construction of interaction network*

180 Cytoscape version 3.6.1 was exerted to construct the networks of lncRNA-mRNA pairs and
181 protein-protein interaction networks with those downloaded files including connected nodes with
182 confidence score.

183 *Statistical analysis*

184 All data were expressed as mean ± standard deviation (SD) unless otherwise noted. The
185 significant difference was measured using a two-tailed student t-test. $P < 0.05$ was considered
186 statistically significant.

Results

The characteristics of rats

The plasma glucose concentration of GK rats was significantly higher than that of control Wistar rats at 3 and 4 weeks of age ($P < 0.001$, Table 1), which was in accordance with previous research (Ando et al. 2018). Besides, the plasma glucose concentration of 3-week-old GK rats was significantly higher than that of 4-week-old GK rats ($P < 0.001$, Table 1).

Differentially expressed lncRNAs and mRNAs

In total, we got 438 and 1000 differentially expressed mRNAs (DEGs) between GK and Wistar rats at 3 and 4 weeks of age, respectively (false discovery rate, FDR < 0.05) (Fig. 2A, Table S3). There were 401 and 746 differentially expressed lncRNAs (DELs) in GK rats compared with Wistar rats at 3 and 4 weeks of age, respectively (FDR < 0.05) (Fig. 2B, Table S4). Among the DEGs, 141 overlapping upregulated mRNAs and 103 overlapping downregulated mRNAs were detected between 3 and 4 weeks (Fig. 2A). A total of 91 overlapping upregulated lncRNAs and 124 overlapping downregulated lncRNAs were found between 3 and 4 weeks (Fig. 2B). From the results of enrichment pathway analysis of DEGs at 3 and 4 weeks, we found the insulin resistance pathway was the only one overlapping pathway between 3 and 4 weeks among top 10 KEGG pathways (Fig. 2C and 2D). The DEGs enriched in insulin resistance pathway were sterol regulatory element binding transcription factor 1 (*Srebf1*, also known as *Srebp1c*), solute carrier family 27 member 1 (*Slc27a1*), protein kinase C, theta (*Prkcq*), cAMP responsive element binding protein 3-like 1 (*Creb3l1*), forkhead box O1 (*Foxo1*), TBC1 domain family, member 4 (*Tbc1d4*, also termed as *AS160*), and carnitine palmitoyltransferase 1A (*Cpt1a*).

To obtain the interaction of the proteins encoded by 141 overlapping upregulated genes and 103 overlapping downregulated genes between 3 and 4 weeks, we analyzed protein-protein interaction of these proteins using STRING. Next, we constructed the protein-protein interaction

network (Fig. 3A and 3B). Then, the top 10 mRNAs according to the node degree among network and their corresponding node degrees were listed in Table S5. The network among top 10 upregulated and downregulated node mRNAs were shown in Fig. 3C and 3D. The dysregulated genes *Srebf1*, *Slc27a1*, *Foxo1* and *Cpt1a* that enriched in insulin resistance pathway also existed in the network of top 10 upregulated and downregulated node mRNAs (Fig. 3C and 3D), which indicating that these four genes might be important for the development of hyperglycemia and T2D in GK rats at the age of 3 and 4 weeks.

The co-expressed lncRNA-mRNA pairs with high correlation coefficients

To investigate the potential function of these DELs, we performed lncRNA-mRNA co-expression network analysis. After filtering, a total of 901 co-expressed lncRNA-mRNA pairs with high correlation coefficients were selected, including 136 DEGs and 120 DELs (Table S6). 136 DEGs were enriched in two KEGG pathways ($P < 0.05$), including transcriptional misregulation in cancer and pathways in cancer. But both pathways were not related to T2D. 136 DEGs were enriched in biological processes (Fig. 4A). Among these DEGs, 2 DEGs (pyruvate dehydrogenase kinase 4, *Pdk4* and *Cpt1a*) were enriched in "regulation of fatty acid oxidation", and 3 DEGs (*Foxo1*, *Pdk4* and *Sh2b2*) were enriched in "insulin receptor signaling pathway". The top 10 nodes ranked by degrees in co-expressed lncRNA-mRNA network were consist of 7 mRNAs and 3 lncRNAs (Table 2). The network of these dysregulated mRNAs (*Cep19*, *Cpt1a*, *Ephx2*, *Foxo1*, *Pdk4*, *Sh2b2* and *Stc2*) and their co-expressed lncRNAs were shown in Fig. 4B. And the expression of key co-expressed lncRNA-mRNA pairs were shown in Fig. 4C and 4D. Notably, the dysregulated genes *Cpt1a*, *Foxo1* and *Pdk4* also appeared in the network of top 10 upregulated and downregulated mRNAs (Fig. 4C and 4D), indicating that these mRNAs might associate with hyperglycemia and T2D in GK rats at the age of 3 and 4 weeks.

However, other genes involved in fatty acid transport and β-oxidation were not significantly dysregulated in GK rats at the age of 3 and 4 weeks (Table S7). In our study, genes related to

glycolysis and glycogen synthesis were not dysregulated in GK rats at 3 and 4 weeks of age (Table S7).

The predicated target mRNAs of differentially expressed lncRNAs

To identify the potential role of dysregulated lncRNAs in the development of hyperglycemia and T2D in GK rats at the age of 3 and 4 weeks, we predicted their cis- and trans-target mRNAs. A total of 15 predicted cis-target DEGs and 88 predicted trans-target DEGs were obtained in DELs at 3 weeks (Table S8). There were 31 predicted cis-target DEGs and 382 predicted trans-target DEGs in DELs at 4 weeks (Table S9). There were 32 overlapping DEL-target DEGs between 3 and 4 weeks (Fig. 5A, Table S10). Network analysis for these overlapping DEGs found out 32 lncRNA-mRNA pairs, including 18 DEGs and 19 DELs (Fig. 5B). Among the 18 DEGs, interleukin 15 (*Il15*), F-box and WD repeat domain containing 7 (*Fbxw7*) and uncoupling protein 3 (*Ucp3*) were related to increased glycaemia (Gray & Kamolrat 2011; Zhao et al. 2018), glucose intolerance (Fujimoto et al. 2019), and increased fatty acid oxidation (Bezaire et al. 2005). Among those 32 lncRNA-target mRNA pairs, 5 lncRNA-target mRNA pairs (NONRATG014028.2-*Pim1*, NONRATG011882.2-*Il15*, NONRATG013497.2-*Fbxw7*, NONRATG011747.2-*Mrps35*, and MSTRG.1662-*Ucp3*) appeared in 901 co-expressed lncRNA-mRNA pairs with high correlation coefficients, suggesting these dysregulated lncRNA-mRNA pairs might involve in the hyperglycemia and T2D of GK rats at the age of 3 and 4 weeks. And the relative expression of NONRATG011882.2-*Il15*, NONRATG013497.2-*Fbxw7*, and MSTRG.1662-*Ucp3* pairs were shown in Fig. 5C.

The target microRNAs (miRNAs) of key DEGs and DELs

To explore the role of lncRNAs in the expression of mRNAs, we predicted the target miRNA of key DELs and DEGs. Then we obtained the overlapping miRNAs targeted both DEGs and DELs in key lncRNA-mRNA pairs (Fig. 6), which provided miRNAs linkers between DELs and DEGs. We found that rno-miR-139-5p, rno-miR-486 and rno-miR-93-5p target both

MSTRG.14356 and *Foxo1* (Fig. 6). We got three target miRNAs rno-miR-20b-5p, rno-miR-27a-3p and rno-miR-17-5p of MSTRG.2584 and *Foxo1* (Fig. 6). The target miRNAs of *Stc2* and MSTRG.2584 were rno-miR-24-3p, rno-miR-532-5p, rno-miR-181a-5p and rno-miR-181b-5p (Fig. 6). MiRNAs rno-miR-195-5p, rno-miR-181b-5p, rno-miR-23b-3p, rno-miR-139-5p and rno-miR-23a-3p were the target miRNAs of MSTRG (Fig. 6).12678 and *Pdk4*. Three miRNAs including rno-miR-34a-5p, rno-miR-125a-5p and rno-miR-125b-5p targeted MSTRG.1662 and *Ucp3* (Fig. 6). Additionally, the target miRNA of NONRATG013497.2 and *Fbxw7* was rno-miR-24-3p (Fig. 6). And rno-miR-326-3p was the target of NONRATG011882.2 and *Il15* (Fig. 6).

Discussion

In the present study, we obtained mRNA and lncRNA expression profiles of skeletal muscle of GK and Wistar rats at 3 and 4 weeks of age by RNA-sequencing. In total, 438 DEGs and 401 DELs were obtained in skeletal muscle of GK rats compared with Wistar rats at the age of 3 weeks (FDR < 0.05), 1000 DEGs and 746 DELs at 4 weeks of age (FDR < 0.05). To address the function of those DELs, we screened the co-expressed lncRNA-mRNA pairs with high correlation coefficients, predicted the target mRNAs of DELs and predicted miRNAs targeted both DEGs and DELs. In considering previous studies, our results indicated that the dysregulated expressed lncRNA-mRNA pairs might be implicated in hyperglycemia, glucose intolerance, and increased fatty acid oxidation in GK rats at the age of 3 and 4 weeks. However, the annotation of lncRNAs is incomplete, and the function of them has not been explained clearly. Thereby, further studies are necessary to reveal their potential function.

The DEGs *Slc27a1*, *Cpt1a*, *Srebf1*, and *Foxo1* were enriched in insulin resistance pathway and also appeared in the network of top 10 upregulated and downregulated mRNAs, indicating these four mRNAs might play key roles in the development of hyperglycemia and T2D in GK rats at the age of 3 and 4 weeks. It has been demonstrated that SLC27A1 was implicated in the regulation of fatty acid transport and oxidation. Overexpression of *Slc27a1* could increase fatty

acid uptake and oxidation in L6E9 skeletal muscle cells (Sebastian et al. 2009). CPT1A encoded by *Cpt1a* is responsible for transport long-chain fatty acid into mitochondria. And overexpression of *Cpt1a* could lead to enhanced fatty acid oxidation in hepatocytes, β-Cells and muscle cells (Akkaoui et al. 2009; Herrero et al. 2005; Perdomo et al. 2004; Stefanovic-Racic et al. 2008). Srebf1 is a transcription factor regulating fatty acid synthesis. The *ob/ob* mice with inactivated SREBF1 showed reduced hepatic fatty acid synthesis (Moon et al. 2012). Blood glucose was significantly higher in *Srebf1*$^{-/-}$ mice than in *Srebf1*$^{+/+}$ mice (Jang et al. 2016). It has been unveiled that inhibiting expression of *Foxo1* could increase glucose oxidation in mouse heart (Gopal et al. 2017). Moreover, TBC1D4 was reported to be involved in glucose uptake. Whole-body knockout *Tbc1d4* mice exhibited markedly decreased insulin-stimulated glucose uptake in skeletal muscle (Lansey et al. 2012; Wang et al. 2013a). Therefore, in our study, the significantly increased expression of *Slc27a1*, *Cpt1a* and *Foxo1* might associate with increased fatty acid transport and oxidation in skeletal muscle of GK rats at 3 and 4 weeks of age. Randle et al pointed out, increased oxidation of fatty acids could repress glucose oxidation (Hue & Taegtmeyer 2009; Randle et al. 1963). Thus, increased fatty acid transport and oxidation might be related to increased glucose concentration in GK rats at the age of 3 and 4 weeks. Additionally, the significantly reduced expression of *Tbc1d4* might be related to decreased glucose uptake in skeletal muscle of GK rats at 3 and 4 weeks of age. Taken together, our results indicated that *Srebf1*, *Slc27a1*, *Foxo1*, *Tbc1d4*, and *Cpt1a* might be related to increased glycaemia in GK rats at 3 and 4 weeks of age.

As GK rats are produced from Wistar rats with impaired glucose tolerance, which plays an essential role in T2D development of GK rats. In this study, *Ephx2*, *Stc2*, *Cep19*, *Il15* and *Fbxw7* genes were found to be associated with impaired glucose tolerance and hyperglycemia. Elevated epoxyeicosatrienoic acids, which was inhibited by the enzyme encoded by *Ephx2*, could improve insulin-stimulated glucose uptake in skeletal muscle of *db/db* mice (Shim et al. 2014). Additionally, previous studies showed that mice with whole-body knockout *Ephx2* exhibited improved insulin secretion (Luo et al. 2010; Luria et al. 2011). Moreover, plasma glucose

clearance was faster in whole-body knockout *Ephx2* mice than that in wild-type mice (Luria et al. 2011). As the expression of *Ephx2* was lower in skeletal muscle than in kidney and liver, the reduced *Ephx2* might have a weaker effect on glucose clearance in skeletal muscle of GK rats at the age of 3 and 4 weeks. Whole-body *Stc2* and *Cep19* knockout mice displayed significantly increased circulating glucose concentration (Lopez et al. 2018), and markedly impaired glucose tolerance and insulin resistant (Shalata et al. 2013), respectively. It has been explored that overexpressed *Il15* transgenic mice showed better glucose tolerance compared to wild-type mice, and Glut4 translocation was promoted in skeletal muscle by AMP-Activated protein kinase pathway (Fujimoto et al. 2019). In addition, skeletal muscle-specific overexpression of *Il15* transgenic mice displayed greater insulin sensitivity and decreased glucose concentration (Quinn et al. 2011). Liver-specific *Fbxw7* knockout mice presented hyperglycemia, glucose intolerance, and insulin resistance (Zhao et al. 2018). Thus, the significantly downregulated *Stc2*, *Il15*, and *Fbxw7* might associate with hyperglycemia and impaired glucose tolerance in GK rats at 3 and 4 weeks of age. Since targeted lncRNAs of these significantly downregulated mRNAs had a high correlation coefficient, the co-expressed pairs lncRNA-mRNA pairs, such as NONRATG003318.2-*Stc2*, NONRATG011882.2-*Il15*, and NONRATG013497.2-*Fbxw7* be related to hyperglycemia and impaired glucose tolerance in GK rats at the age of 3 and 4 weeks.

It is well known that increased fatty acid oxidation could inhibit glucose oxidation in heart and skeletal muscle (Hue & Taegtmeyer 2009; Randle et al. 1963). Thus, the dysregulated fatty acid oxidation might affect circulating glucose concentration. *Pdk4* and *Ucp3* were found to be associated with increased fatty acid oxidation. Upregulated *Pdk4* could decrease glucose oxidation and enhance fatty acid oxidation in myocardium and skeletal muscle (Sugden & Holness 2003; Zhao et al. 2008). As one transcriptional factor, Foxo1 could regulate the expression of *Pdk4*, and the inhibition of it could increase glucose oxidation in mouse heart (Gopal et al. 2017). Ucp3, located in mitochondrial inner membrane, expressed predominantly of skeletal muscle in humans and rodents (Boss et al. 1997). Whole-body *Ucp3* overexpression mice showed increased activity of enzymes that implicated in fatty acid oxidation in skeletal

muscle (Bezaire et al. 2005). The significantly decreased rate of long-chain fatty acid oxidation was observed in rat heart with partial loss of *Ucp3* gene ($Ucp3^{+/-}$) (Edwards et al. 2018). Hence, in our study, the significantly increased *Pdk4*, and *Ucp3* and their corresponding co-expressed or targeted lncRNAs, including NONRATG017315.2-*Pdk4*, and MSTRG.1662-*Ucp3* might contribute to increased glycaemia and increased fatty acid oxidation in GK rats at 3 and 4 weeks of age.

Glycolysis and glycogen synthesis were demonstrated to be involved in glucose homeostasis (Hwang et al. 1995; Rothman et al. 1992; Shulman et al. 1990). However, in our study, genes related to glycolysis and glycogen synthase were not dysregulated in GK rats at the age of 3 and 4 weeks.

Recently, evidences showed that lncRNAs could regulate mRNAs by interacting with microRNAs (miRNAs) (Zhang & Zhu 2014). Among the target miRNA of mRNAs we predicted, miR-139 has been identified could target *Foxo1* directly and inhibit its expression in mice hepatocytes (Hasseine et al. 2009). What's more, miR-139 overexpression leads to markedly reduced *Foxo1* level, and the inhibition of miR-139 contribute to increased *Foxo1* level (Yan et al. 2018). Moreover, *Foxo1* was the target gene of miR-486-5p (Liu et al. 2019). Thus, the DELs in key lncRNA-mRNA pairs might regulate mRNAs level through binding to their common miRNAs. Further studies are needed to identify the target miRNAs of DEGs and DELs and measure the miRNAs profiles in skeletal muscle of GK rats in the future.

Conclusions

In the present study, we found that the dysregulated lncARNA-mRNA pairs (NONRATG017315.2-*Pdk4*, NONRATG003318.2-*Stc2*, NONRATG011882.2-*Il15*, NONRATG013497.2-*Fbxw7* and MSTRG.1662-*Ucp3*) might be implicated in hyperglycemia, glucose intolerance, as well as dysregulated glucose and fatty acid oxidation in GK rats at 3 and 4 weeks of age. These results may provide more comprehensive knowledge about mRNAs and lncRNAs in skeletal muscle of GK rats at the age of 3 and 4 weeks. Furthermore, these results

may serve as important resources for future studies to investigate the regulatory mechanism of lncRNAs in skeletal muscle of GK rats at the age of 3 and 4 weeks.

References

Agarwal V, Bell GW, Nam JW, and Bartel DP. 2015. Predicting effective microRNA target sites in mammalian mRNAs. *Elife* 4. 10.7554/eLife.05005

Akerman I, Tu Z, Beucher A, Rolando DMY, Sauty-Colace C, Benazra M, Nakic N, Yang J, Wang H, Pasquali L, Moran I, Garcia-Hurtado J, Castro N, Gonzalez-Franco R, Stewart AF, Bonner C, Piemonti L, Berney T, Groop L, Kerr-Conte J, Pattou F, Argmann C, Schadt E, Ravassard P, and Ferrer J. 2017. Human Pancreatic beta Cell lncRNAs Control Cell-Specific Regulatory Networks. *Cell Metab* 25:400-411. 10.1016/j.cmet.2016.11.016

Akkaoui M, Cohen I, Esnous C, Lenoir V, Sournac M, Girard J, and Prip-Buus C. 2009. Modulation of the hepatic malonyl-CoA-carnitine palmitoyltransferase 1A partnership creates a metabolic switch allowing oxidation of de novo fatty acids. *Biochem J* 420:429-438. 10.1042/BJ20081932

Almon RR, Dubois DC, Sukumaran S, Wang X, Xue B, Nie J, and Jusko WJ. 2012. Effects of high fat feeding on liver gene expression in diabetic goto-kakizaki rats. *Gene Regul Syst Bio* 6:151-168. 10.4137/GRSB.S10371

Ando A, Gantulga D, Nakata M, Maekawa F, Dezaki K, Ishibashi S, and Yada T. 2018. Weaning stage hyperglycemia induces glucose-insensitivity in arcuate POMC neurons and hyperphagia in type 2 diabetic GK rats. *Neuropeptides* 68:49-56. 10.1016/j.npep.2018.02.001

Baron AD, Brechtel G, Wallace P, and Edelman SV. 1988. Rates and tissue sites of non-insulin- and insulin-mediated glucose uptake in humans. *Am J Physiol* 255:E769-774. 10.1152/ajpendo.1988.255.6.E769

Bezaire V, Spriet LL, Campbell S, Sabet N, Gerrits M, Bonen A, and Harper ME. 2005. Constitutive UCP3 overexpression at physiological levels increases mouse skeletal muscle capacity for fatty acid transport and oxidation. *FASEB J* 19:977-979. 10.1096/fj.04-2765fje

Bisbis S, Bailbe D, Tormo MA, Picarel-Blanchot F, Derouet M, Simon J, and Portha B. 1993. Insulin resistance in the GK rat: decreased receptor number but normal kinase activity in liver. *Am J Physiol* 265:E807-813. 10.1152/ajpendo.1993.265.5.E807

Boss O, Samec S, Paoloni-Giacobino A, Rossier C, Dulloo A, Seydoux J, Muzzin P, and Giacobino JP. 1997. Uncoupling protein-3: a new member of the mitochondrial carrier family with tissue-specific expression. *FEBS Lett* 408:39-42.

Cabili MN, Trapnell C, Goff L, Koziol M, Tazon-Vega B, Regev A, and Rinn JL. 2011. Integrative annotation of human large intergenic noncoding RNAs reveals global properties and specific subclasses. *Genes Dev* 25:1915-1927. 10.1101/gad.17446611

Dadke SS, Li HC, Kusari AB, Begum N, and Kusari J. 2000. Elevated expression and activity of protein-tyrosine phosphatase 1B in skeletal muscle of insulin-resistant type II diabetic Goto-Kakizaki rats. *Biochem Biophys Res Commun* 274:583-589. 10.1006/bbrc.2000.3188

DeFronzo RA, Jacot E, Jequier E, Maeder E, Wahren J, and Felber JP. 1981. The effect of insulin on the disposal of intravenous glucose. Results from indirect calorimetry and hepatic and femoral venous catheterization. *Diabetes* 30:1000-1007.

Derrien T, Johnson R, Bussotti G, Tanzer A, Djebali S, Tilgner H, Guernec G, Martin D, Merkel A, Knowles DG, Lagarde J, Veeravalli L, Ruan X, Ruan Y, Lassmann T, Carninci P, Brown JB, Lipovich L, Gonzalez JM, Thomas M, Davis CA, Shiekhattar R, Gingeras TR, Hubbard TJ, Notredame C, Harrow J, and Guigo R. 2012. The GENCODE v7 catalog of human long noncoding RNAs: analysis of their gene structure, evolution, and expression. *Genome Res* 22:1775-1789. 10.1101/gr.132159.111

Djebali S, Davis CA, Merkel A, Dobin A, Lassmann T, Mortazavi A, Tanzer A, Lagarde J, Lin W, Schlesinger F, Xue C, Marinov GK, Khatun J, Williams BA, Zaleski C, Rozowsky J, Roder M, Kokocinski F, Abdelhamid RF, Alioto T, Antoshechkin I, Baer MT, Bar NS, Batut P, Bell K, Bell I, Chakrabortty S, Chen X, Chrast J, Curado J, Derrien T, Drenkow J, Dumais E, Dumais J, Duttagupta R, Falconnet E, Fastuca M, Fejes-Toth K, Ferreira P, Foissac S, Fullwood MJ, Gao H, Gonzalez D, Gordon A, Gunawardena H, Howald C, Jha S, Johnson R, Kapranov P, King B, Kingswood C, Luo OJ, Park E, Persaud K, Preall JB, Ribeca P, Risk B, Robyr D, Sammeth M, Schaffer L, See LH, Shahab A, Skancke J, Suzuki AM, Takahashi H, Tilgner H, Trout D, Walters N, Wang H, Wrobel J, Yu Y, Ruan X, Hayashizaki Y, Harrow J, Gerstein M, Hubbard T, Reymond A, Antonarakis SE, Hannon G, Giddings MC, Ruan Y, Wold B, Carninci P, Guigo R, and Gingeras TR. 2012. Landscape of transcription in human cells. *Nature* 489:101-108. 10.1038/nature11233

Dobin A, and Gingeras TR. 2015. Mapping RNA-seq Reads with STAR. *Curr Protoc Bioinformatics* 51:11 14 11-19. 10.1002/0471250953.bi1114s51

Edwards KS, Ashraf S, Lomax TM, Wiseman JM, Hall ME, Gava FN, Hall JE, Hosler JP, and Harmancey R. 2018. Uncoupling protein 3 deficiency impairs myocardial fatty acid oxidation and contractile recovery following ischemia/reperfusion. *Basic Res Cardiol* 113:47. 10.1007/s00395-018-0707-9

Espinoza CA, Allen TA, Hieb AR, Kugel JF, and Goodrich JA. 2004. B2 RNA binds directly to RNA polymerase II to repress transcript synthesis. *Nat Struct Mol Biol* 11:822-829. 10.1038/nsmb812

Esteller M. 2011. Non-coding RNAs in human disease. *Nat Rev Genet* 12:861-874. 10.1038/nrg3074

Frazee AC, Pertea G, Jaffe AE, Langmead B, Salzberg SL, and Leek JT. 2015. Ballgown bridges the gap between transcriptome assembly and expression analysis. *Nat Biotechnol* 33:243-246. 10.1038/nbt.3172

Fujimoto T, Sugimoto K, Takahashi T, Yasunobe Y, Xie K, Tanaka M, Ohnishi Y, Yoshida S, Kurinami H, Akasaka H, Takami Y, Takeya Y, Yamamoto K, and Rakugi H. 2019. Overexpression of Interleukin-15 exhibits improved glucose tolerance and promotes GLUT4 translocation via AMP-Activated protein kinase pathway in skeletal muscle. *Biochem Biophys Res Commun* 509:994-1000. 10.1016/j.bbrc.2019.01.024

Gao Y, Wu F, Zhou J, Yan L, Jurczak MJ, Lee HY, Yang L, Mueller M, Zhou XB, Dandolo L, Szendroedi J, Roden M, Flannery C, Taylor H, Carmichael GG, Shulman GI, and Huang Y. 2014. The H19/let-7 double-negative feedback loop contributes to glucose metabolism in muscle cells. *Nucleic Acids Res* 42:13799-13811. 10.1093/nar/gku1160

Gopal K, Saleme B, Al Batran R, Aburasayn H, Eshreif A, Ho KL, Ma WK, Almutairi M, Eaton F, Gandhi M, Park EA, Sutendra G, and Ussher JR. 2017. FoxO1 regulates myocardial glucose oxidation rates via transcriptional control of pyruvate dehydrogenase kinase 4 expression. *Am J Physiol Heart Circ Physiol* 313:H479-H490. 10.1152/ajpheart.00191.2017

Goto Y, Kakizaki M, and Masaki N. 1976. Production of spontaneous diabetic rats by repetition of selective breeding. *Tohoku J Exp Med* 119:85-90.

Gray SR, and Kamolrat T. 2011. The effect of exercise induced cytokines on insulin stimulated glucose transport in C2C12 cells. *Cytokine* 55:221-228. 10.1016/j.cyto.2011.04.019

446 Guil S, and Esteller M. 2012. Cis-acting noncoding RNAs: friends and foes. *Nat Struct Mol Biol* 19:1068-1075.
447 10.1038/nsmb.2428
448 Guttman M, and Rinn JL. 2012. Modular regulatory principles of large non-coding RNAs. *Nature* 482:339-346.
449 10.1038/nature10887
450 Hasseine LK, Hinault C, Lebrun P, Gautier N, Paul-Bellon R, and Van Obberghen E. 2009. miR-139 impacts FoxO1
451 action by decreasing FoxO1 protein in mouse hepatocytes. *Biochem Biophys Res Commun* 390:1278-1282.
452 10.1016/j.bbrc.2009.10.135
453 Herrero L, Rubi B, Sebastian D, Serra D, Asins G, Maechler P, Prentki M, and Hegardt FG. 2005. Alteration of the
454 malonyl-CoA/carnitine palmitoyltransferase I interaction in the beta-cell impairs glucose-induced insulin
455 secretion. *Diabetes* 54:462-471.
456 Hue L, and Taegtmeyer H. 2009. The Randle cycle revisited: a new head for an old hat. *Am J Physiol Endocrinol*
457 *Metab* 297:E578-591. 10.1152/ajpendo.00093.2009
458 Hwang JH, Perseghin G, Rothman DL, Cline GW, Magnusson I, Petersen KF, and Shulman GI. 1995. Impaired net
459 hepatic glycogen synthesis in insulin-dependent diabetic subjects during mixed meal ingestion. A 13C
460 nuclear magnetic resonance spectroscopy study. *J Clin Invest* 95:783-787. 10.1172/JCI117727
461 Jang H, Lee GY, Selby CP, Lee G, Jeon YG, Lee JH, Cheng KK, Titchenell P, Birnbaum MJ, Xu A, Sancar A, and Kim JB.
462 2016. SREBP1c-CRY1 signalling represses hepatic glucose production by promoting FOXO1 degradation
463 during refeeding. *Nat Commun* 7:12180. 10.1038/ncomms12180
464 Jia H, Osak M, Bogu GK, Stanton LW, Johnson R, and Lipovich L. 2010. Genome-wide computational identification
465 and manual annotation of human long noncoding RNA genes. *RNA* 16:1478-1487. 10.1261/rna.1951310
466 Kang YJ, Yang DC, Kong L, Hou M, Meng YQ, Wei L, and Gao G. 2017. CPC2: a fast and accurate coding potential
467 calculator based on sequence intrinsic features. *Nucleic Acids Res* 45:W12-W16. 10.1093/nar/gkx428
468 Kayala MA, and Baldi P. 2012. Cyber-T web server: differential analysis of high-throughput data. *Nucleic Acids Res*
469 40:W553-559. 10.1093/nar/gks420
470 Kitahara A, Toyota T, Kakizaki M, and Goto Y. 1978. Activities of hepatic enzymes in spontaneous diabetes rats
471 produced by selective breeding of normal Wistar rats. *Tohoku J Exp Med* 126:7-11.
472 Lansey MN, Walker NN, Hargett SR, Stevens JR, and Keller SR. 2012. Deletion of Rab GAP AS160 modifies glucose
473 uptake and GLUT4 translocation in primary skeletal muscles and adipocytes and impairs glucose
474 homeostasis. *Am J Physiol Endocrinol Metab* 303:E1273-1286. 10.1152/ajpendo.00316.2012
475 Liang Y, Yu B, Wang Y, Qiao Z, Cao T, and Zhang P. 2017. Duodenal long noncoding RNAs are associated with
476 glycemic control after bariatric surgery in high-fat diet-induced diabetic mice. *Surg Obes Relat Dis*
477 13:1212-1226. 10.1016/j.soard.2017.02.010
478 Liu H, Ni Z, Shi L, Ma L, and Zhao J. 2019. MiR-486-5p inhibits the proliferation of leukemia cells and induces
479 apoptosis through targeting FOXO1. *Mol Cell Probes* 44:37-43. 10.1016/j.mcp.2019.02.001
480 Liu JY, Yao J, Li XM, Song YC, Wang XQ, Li YJ, Yan B, and Jiang Q. 2014. Pathogenic role of lncRNA-MALAT1 in
481 endothelial cell dysfunction in diabetes mellitus. *Cell Death Dis* 5:e1506. 10.1038/cddis.2014.466
482 Lopez JJ, Jardin I, Cantonero Chamorro C, Duran ML, Tarancon Rubio MJ, Reyes Panadero M, Jimenez F, Montero R,
483 Gonzalez MJ, Martinez M, Hernandez MJ, Brull JM, Corbacho AJ, Delgado E, Granados MP, Gomez-Gordo
484 L, Rosado JA, and Redondo PC. 2018. Involvement of stanniocalcins in the deregulation of glycaemia in
485 obese mice and type 2 diabetic patients. *J Cell Mol Med* 22:684-694. 10.1111/jcmm.13355

Luo P, Chang HH, Zhou Y, Zhang S, Hwang SH, Morisseau C, Wang CY, Inscho EW, Hammock BD, and Wang MH. 2010. Inhibition or deletion of soluble epoxide hydrolase prevents hyperglycemia, promotes insulin secretion, and reduces islet apoptosis. *J Pharmacol Exp Ther* 334:430-438. 10.1124/jpet.110.167544

Luo Q, and Chen Y. 2016. Long noncoding RNAs and Alzheimer's disease. *Clin Interv Aging* 11:867-872. 10.2147/CIA.S107037

Luria A, Bettaieb A, Xi Y, Shieh GJ, Liu HC, Inoue H, Tsai HJ, Imig JD, Haj FG, and Hammock BD. 2011. Soluble epoxide hydrolase deficiency alters pancreatic islet size and improves glucose homeostasis in a model of insulin resistance. *Proc Natl Acad Sci U S A* 108:9038-9043. 10.1073/pnas.1103482108

Mercer TR, Dinger ME, Sunkin SM, Mehler MF, and Mattick JS. 2008. Specific expression of long noncoding RNAs in the mouse brain. *Proc Natl Acad Sci U S A* 105:716-721. 10.1073/pnas.0706729105

Moon YA, Liang G, Xie X, Frank-Kamenetsky M, Fitzgerald K, Koteliansky V, Brown MS, Goldstein JL, and Horton JD. 2012. The Scap/SREBP pathway is essential for developing diabetic fatty liver and carbohydrate-induced hypertriglyceridemia in animals. *Cell Metab* 15:240-246. 10.1016/j.cmet.2011.12.017

Moran I, Akerman I, van de Bunt M, Xie R, Benazra M, Nammo T, Arnes L, Nakic N, Garcia-Hurtado J, Rodriguez-Segui S, Pasquali L, Sauty-Colace C, Beucher A, Scharfmann R, van Arensbergen J, Johnson PR, Berry A, Lee C, Harkins T, Gmyr V, Pattou F, Kerr-Conte J, Piemonti L, Berney T, Hanley N, Gloyn AL, Sussel L, Langman L, Brayman KL, Sander M, McCarthy MI, Ravassard P, and Ferrer J. 2012. Human beta cell transcriptome analysis uncovers lncRNAs that are tissue-specific, dynamically regulated, and abnormally expressed in type 2 diabetes. *Cell Metab* 16:435-448. 10.1016/j.cmet.2012.08.010

Nie J, DuBois DC, Xue B, Jusko WJ, and Almon RR. 2017. Effects of High-Fat Feeding on Skeletal Muscle Gene Expression in Diabetic Goto-Kakizaki Rats. *Gene Regul Syst Bio* 11:1177625017710009. 10.1177/1177625017710009

Nie J, Xue B, Sukumaran S, Jusko WJ, Dubois DC, and Almon RR. 2011. Differential muscle gene expression as a function of disease progression in Goto-Kakizaki diabetic rats. *Mol Cell Endocrinol* 338:10-17. 10.1016/j.mce.2011.02.016

Perdomo G, Commerford SR, Richard AM, Adams SH, Corkey BE, O'Doherty RM, and Brown NF. 2004. Increased beta-oxidation in muscle cells enhances insulin-stimulated glucose metabolism and protects against fatty acid-induced insulin resistance despite intramyocellular lipid accumulation. *J Biol Chem* 279:27177-27186. 10.1074/jbc.M403566200

Pertea M, Pertea GM, Antonescu CM, Chang TC, Mendell JT, and Salzberg SL. 2015. StringTie enables improved reconstruction of a transcriptome from RNA-seq reads. *Nat Biotechnol* 33:290-295. 10.1038/nbt.3122

Peterlin BM, Brogie JE, and Price DH. 2012. 7SK snRNA: a noncoding RNA that plays a major role in regulating eukaryotic transcription. *Wiley Interdiscip Rev RNA* 3:92-103. 10.1002/wrna.106

Portha B, Giroix MH, Tourrel-Cuzin C, Le-Stunff H, and Movassat J. 2012. The GK rat: a prototype for the study of non-overweight type 2 diabetes. *Methods Mol Biol* 933:125-159. 10.1007/978-1-62703-068-7_9

Quinn LS, Anderson BG, Conner JD, Pistilli EE, and Wolden-Hanson T. 2011. Overexpression of interleukin-15 in mice promotes resistance to diet-induced obesity, increased insulin sensitivity, and markers of oxidative skeletal muscle metabolism. *Int J Interferon Cytokine Mediat Res* 3:29-42. 10.2147/IJICMR.S19007

Randle PJ, Garland PB, Hales CN, and Newsholme EA. 1963. The glucose fatty-acid cycle. Its role in insulin sensitivity and the metabolic disturbances of diabetes mellitus. *Lancet* 1:785-789.

526 Reddy MA, Chen Z, Park JT, Wang M, Lanting L, Zhang Q, Bhatt K, Leung A, Wu X, Putta S, Saetrom P, Devaraj S, and
527 Natarajan R. 2014. Regulation of inflammatory phenotype in macrophages by a diabetes-induced long
528 noncoding RNA. *Diabetes* 63:4249-4261. 10.2337/db14-0298
529 Rehmsmeier M, Steffen P, Hochsmann M, and Giegerich R. 2004. Fast and effective prediction of microRNA/target
530 duplexes. *RNA* 10:1507-1517. 10.1261/rna.5248604
531 Rinn JL, Kertesz M, Wang JK, Squazzo SL, Xu X, Brugmann SA, Goodnough LH, Helms JA, Farnham PJ, Segal E, and
532 Chang HY. 2007. Functional demarcation of active and silent chromatin domains in human HOX loci by
533 noncoding RNAs. *Cell* 129:1311-1323. 10.1016/j.cell.2007.05.022
534 Rothman DL, Shulman RG, and Shulman GI. 1992. 31P nuclear magnetic resonance measurements of muscle
535 glucose-6-phosphate. Evidence for reduced insulin-dependent muscle glucose transport or
536 phosphorylation activity in non-insulin-dependent diabetes mellitus. *J Clin Invest* 89:1069-1075.
537 10.1172/JCI115686
538 Sebastian D, Guitart M, Garcia-Martinez C, Mauvezin C, Orellana-Gavalda JM, Serra D, Gomez-Foix AM, Hegardt
539 FG, and Asins G. 2009. Novel role of FATP1 in mitochondrial fatty acid oxidation in skeletal muscle cells. *J*
540 *Lipid Res* 50:1789-1799. 10.1194/jlr.M800535-JLR200
541 Shalata A, Ramirez MC, Desnick RJ, Priedigkeit N, Buettner C, Lindtner C, Mahroum M, Abdul-Ghani M, Dong F,
542 Arar N, Camacho-Vanegas O, Zhang R, Camacho SC, Chen Y, Ibdah M, DeFronzo R, Gillespie V, Kelley K,
543 Dynlacht BD, Kim S, Glucksman MJ, Borochowitz ZU, and Martignetti JA. 2013. Morbid obesity resulting
544 from inactivation of the ciliary protein CEP19 in humans and mice. *Am J Hum Genet* 93:1061-1071.
545 10.1016/j.ajhg.2013.10.025
546 Shim CY, Kim S, Chadderdon S, Wu M, Qi Y, Xie A, Alkayed NJ, Davidson BP, and Lindner JR. 2014.
547 Epoxyeicosatrienoic acids mediate insulin-mediated augmentation in skeletal muscle perfusion and blood
548 volume. *Am J Physiol Endocrinol Metab* 307:E1097-1104. 10.1152/ajpendo.00216.2014
549 Shulman GI, Rothman DL, Jue T, Stein P, DeFronzo RA, and Shulman RG. 1990. Quantitation of muscle glycogen
550 synthesis in normal subjects and subjects with non-insulin-dependent diabetes by 13C nuclear magnetic
551 resonance spectroscopy. *N Engl J Med* 322:223-228. 10.1056/NEJM199001253220403
552 Stefanovic-Racic M, Perdomo G, Mantell BS, Sipula IJ, Brown NF, and O'Doherty RM. 2008. A moderate increase in
553 carnitine palmitoyltransferase 1a activity is sufficient to substantially reduce hepatic triglyceride levels.
554 *Am J Physiol Endocrinol Metab* 294:E969-977. 10.1152/ajpendo.00497.2007
555 Steiler TL, Galuska D, Leng Y, Chibalin AV, Gilbert M, and Zierath JR. 2003. Effect of hyperglycemia on signal
556 transduction in skeletal muscle from diabetic Goto-Kakizaki rats. *Endocrinology* 144:5259-5267.
557 10.1210/en.2003-0447
558 Sugden MC, and Holness MJ. 2003. Recent advances in mechanisms regulating glucose oxidation at the level of the
559 pyruvate dehydrogenase complex by PDKs. *Am J Physiol Endocrinol Metab* 284:E855-862.
560 10.1152/ajpendo.00526.2002
561 Sun L, Luo H, Bu D, Zhao G, Yu K, Zhang C, Liu Y, Chen R, and Zhao Y. 2013. Utilizing sequence intrinsic composition
562 to classify protein-coding and long non-coding transcripts. *Nucleic Acids Res* 41:e166. 10.1093/nar/gkt646
563 Szklarczyk D, Franceschini A, Kuhn M, Simonovic M, Roth A, Minguez P, Doerks T, Stark M, Muller J, Bork P, Jensen
564 LJ, and von Mering C. 2011. The STRING database in 2011: functional interaction networks of proteins,
565 globally integrated and scored. *Nucleic Acids Res* 39:D561-568. 10.1093/nar/gkq973

566 Tsoi LC, Iyer MK, Stuart PE, Swindell WR, Gudjonsson JE, Tejasvi T, Sarkar MK, Li B, Ding J, Voorhees JJ, Kang HM,
567 Nair RP, Chinnaiyan AM, Abecasis GR, and Elder JT. 2015. Analysis of long non-coding RNAs highlights
568 tissue-specific expression patterns and epigenetic profiles in normal and psoriatic skin. *Genome Biol*
569 16:24. 10.1186/s13059-014-0570-4
570 Wang HY, Ducommun S, Quan C, Xie B, Li M, Wasserman DH, Sakamoto K, Mackintosh C, and Chen S. 2013a. AS160
571 deficiency causes whole-body insulin resistance via composite effects in multiple tissues. *Biochem J*
572 449:479-489. 10.1042/BJ20120702
573 Wang L, Park HJ, Dasari S, Wang S, Kocher JP, and Li W. 2013b. CPAT: Coding-Potential Assessment Tool using an
574 alignment-free logistic regression model. *Nucleic Acids Res* 41:e74. 10.1093/nar/gkt006
575 Xue B, Sukumaran S, Nie J, Jusko WJ, Dubois DC, and Almon RR. 2011. Adipose tissue deficiency and chronic
576 inflammation in diabetic Goto-Kakizaki rats. *PLoS One* 6:e17386. 10.1371/journal.pone.0017386
577 Yan C, Li J, Feng S, Li Y, and Tan L. 2018. Long noncoding RNA Gomafu upregulates Foxo1 expression to promote
578 hepatic insulin resistance by sponging miR-139-5p. *Cell Death Dis* 9:289. 10.1038/s41419-018-0321-7
579 Yin DD, Zhang EB, You LH, Wang N, Wang LT, Jin FY, Zhu YN, Cao LH, Yuan QX, De W, and Tang W. 2015.
580 Downregulation of lncRNA TUG1 affects apoptosis and insulin secretion in mouse pancreatic beta cells.
581 *Cell Physiol Biochem* 35:1892-1904. 10.1159/000373999
582 You L, Wang N, Yin D, Wang L, Jin F, Zhu Y, Yuan Q, and De W. 2016. Downregulation of Long Noncoding RNA Meg3
583 Affects Insulin Synthesis and Secretion in Mouse Pancreatic Beta Cells. *J Cell Physiol* 231:852-862.
584 10.1002/jcp.25175
585 Zhang H, and Zhu JK. 2014. Emerging roles of RNA processing factors in regulating long non-coding RNAs. *RNA Biol*
586 11:793-797. 10.4161/rna.29731
587 Zhao G, Jeoung NH, Burgess SC, Rosaaen-Stowe KA, Inagaki T, Latif S, Shelton JM, McAnally J, Bassel-Duby R, Harris
588 RA, Richardson JA, and Kliewer SA. 2008. Overexpression of pyruvate dehydrogenase kinase 4 in heart
589 perturbs metabolism and exacerbates calcineurin-induced cardiomyopathy. *Am J Physiol Heart Circ*
590 *Physiol* 294:H936-943. 10.1152/ajpheart.00870.2007
591 Zhao J, Xiong X, Li Y, Liu X, Wang T, Zhang H, Jiao Y, Jiang J, Zhang H, Tang Q, Gao X, Li X, Lu Y, Liu B, Hu C, and Li X.
592 2018. Hepatic F-Box Protein FBXW7 Maintains Glucose Homeostasis Through Degradation of Fetuin-A.
593 *Diabetes* 67:818-830. 10.2337/db17-1348
594 Zhu X, Wu YB, Zhou J, and Kang DM. 2016. Upregulation of lncRNA MEG3 promotes hepatic insulin resistance via
595 increasing FoxO1 expression. *Biochem Biophys Res Commun* 469:319-325. 10.1016/j.bbrc.2015.11.048

596

Figure 1

Figure 1 Flowchart of data analysis pipeline.

FDR: false discovery rate. DEGs: differentially expressed mRNAs; DELs: differentially expressed lncRNAs; PPI: protein-protein interaction. GO: Gene Ontology; KEGG: Kyoto Encyclopedia of Genes and Genomes.

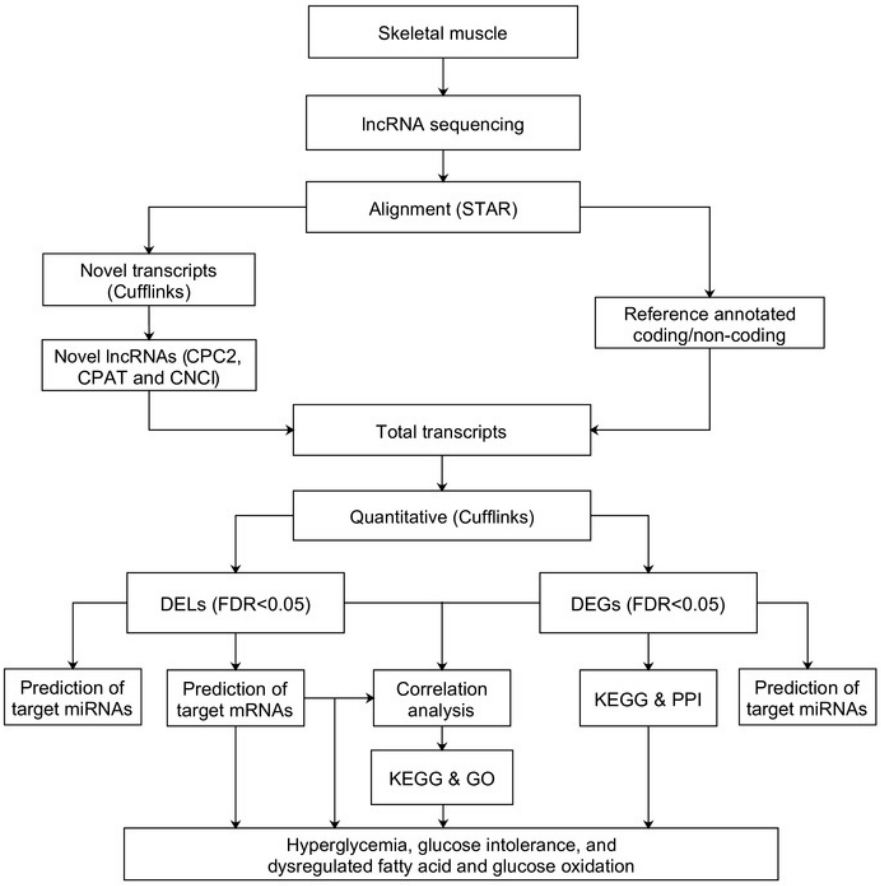

Figure 2

Figure 2 The differentially expressed lncRNAs and mRNAs in skeletal muscle of GK rats compared with aged-matched Wistar rats.

(A) Venn diagram of differentially expressed mRNAs (DEGs) in skeletal muscle of GK rats compared with aged-matched Wistar rats at the age of 3 and 4 weeks. (B) Venn diagram of differentially expressed lncRNAs (DELs) in skeletal muscle of GK rats compared with aged-matched Wistar rats at the age of 3 and 4 weeks. (C) The top 10 KEGG pathways of DEGs in GK rats compared with aged-matched Wistar rats at the age of 3 weeks. (D) The top 10 KEGG pathways of DEGs in GK rats compared with aged-matched Wistar rats at the age of 4 weeks. The 3wk_up_DEGs represents upregulated mRNAs at 3 weeks. The 4wk_up_DEGs represents upregulated mRNAs at 4 weeks. The 3wk_down_DEGs represents downregulated mRNAs at 3 weeks. The 4wk_down_DEGs represents downregulated mRNAs at 4 weeks. The 3wk_up_DELs represents upregulated lncRNAs at 3 weeks. The 4wk_up_DELs represents upregulated lncRNAs at 4 weeks. The 3wk_down_DELs represents downregulated lncRNAs at 3 weeks. The 4wk_down_DELs represents downregulated lncRNAs at 4 weeks.

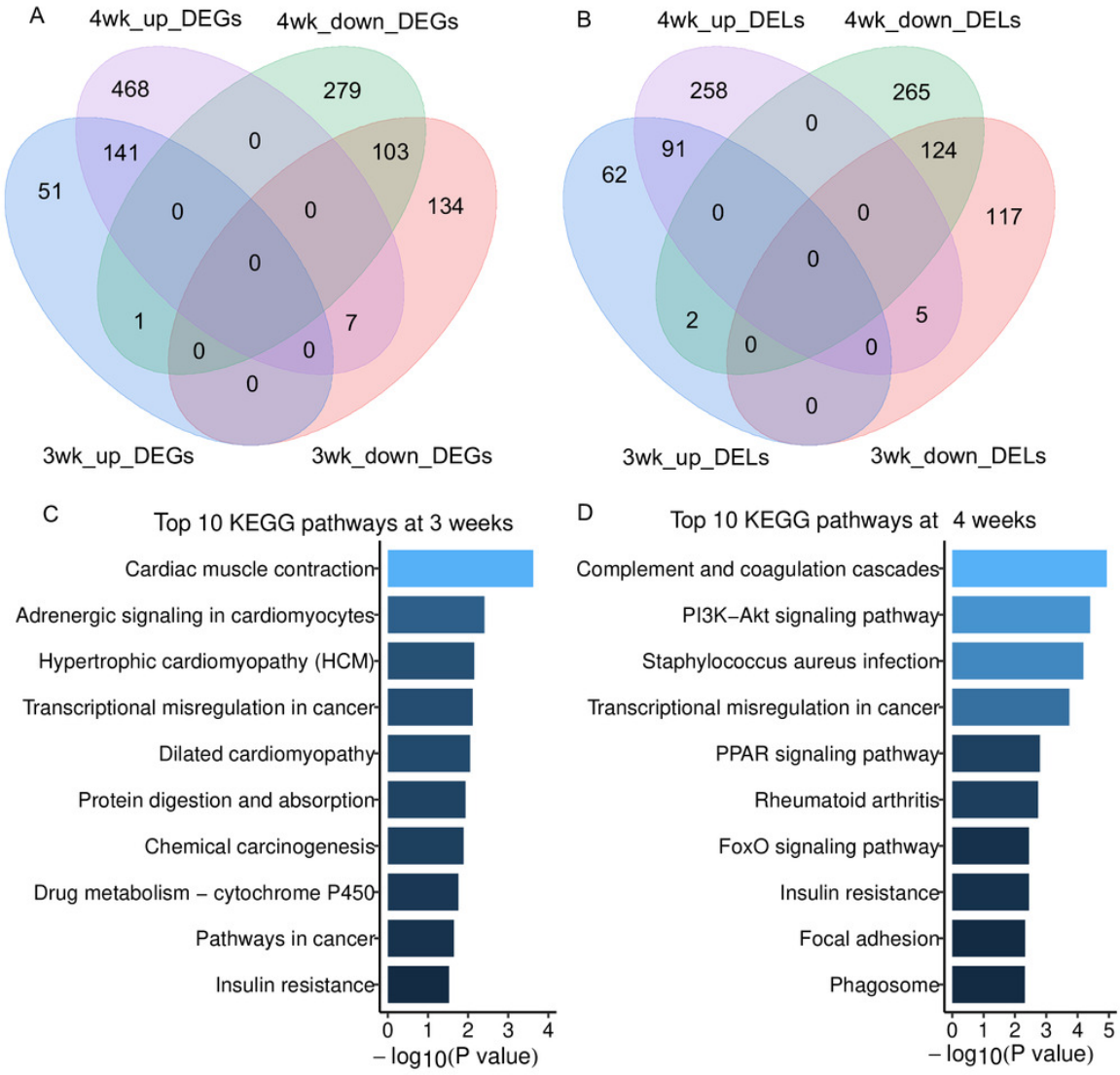
A
4wk_up_DEGs
4wk_down_DEGs
468
279
141
0
103
51
0
0
134
0
1
7
0
0
0
3wk_up_DEGs
3wk_down_DEGs
B
4wk_up_DELs
4wk_down_DELs
258
265
0
91
124
62
0
0
117
0
2
5
0
0
0
3wk_up_DELs
3wk_down_DELs
C
Top 10 KEGG pathways at 3 weeks
Cardiac muscle contraction
Adrenergic signaling in cardiomyocytes
Hypertrophic cardiomyopathy (HCM)
Transcriptional misregulation in cancer
Dilated cardiomyopathy
Protein digestion and absorption
Chemical carcinogenesis
Drug metabolism – cytochrome P450
Pathways in cancer
Insulin resistance
0 1 2 3 4
– log10(P value)
D
Top 10 KEGG pathways at 4 weeks
Complement and coagulation cascades
PI3K–Akt signaling pathway
Staphylococcus aureus infection
Transcriptional misregulation in cancer
PPAR signaling pathway
Rheumatoid arthritis
FoxO signaling pathway
Insulin resistance
Focal adhesion
Phagosome
0 1 2 3 4 5
– log10(P value)

Figure 3

Figure 3 The top 10 mRNAs identified in protein-protein interaction networks.

(A) The protein-protein interaction network of overlapping upregulated DEGs at 3 and 4 weeks. The red represents significantly upregulated mRNAs in GK rats at the age of 3 and 4 weeks. (B) The protein-protein interaction network of overlapping downregulated DEGs at 3 and 4 weeks. The blue represents significantly downregulated mRNAs in GK rats at the age of 3 and 4 weeks. (C) The top 10 upregulated mRNAs ranked by node degree. The darker of the color indicates the higher of connectivity degree. (D) The top 10 downregulated mRNAs ranked by node degree. The darker of the color indicates the higher of connectivity degree.

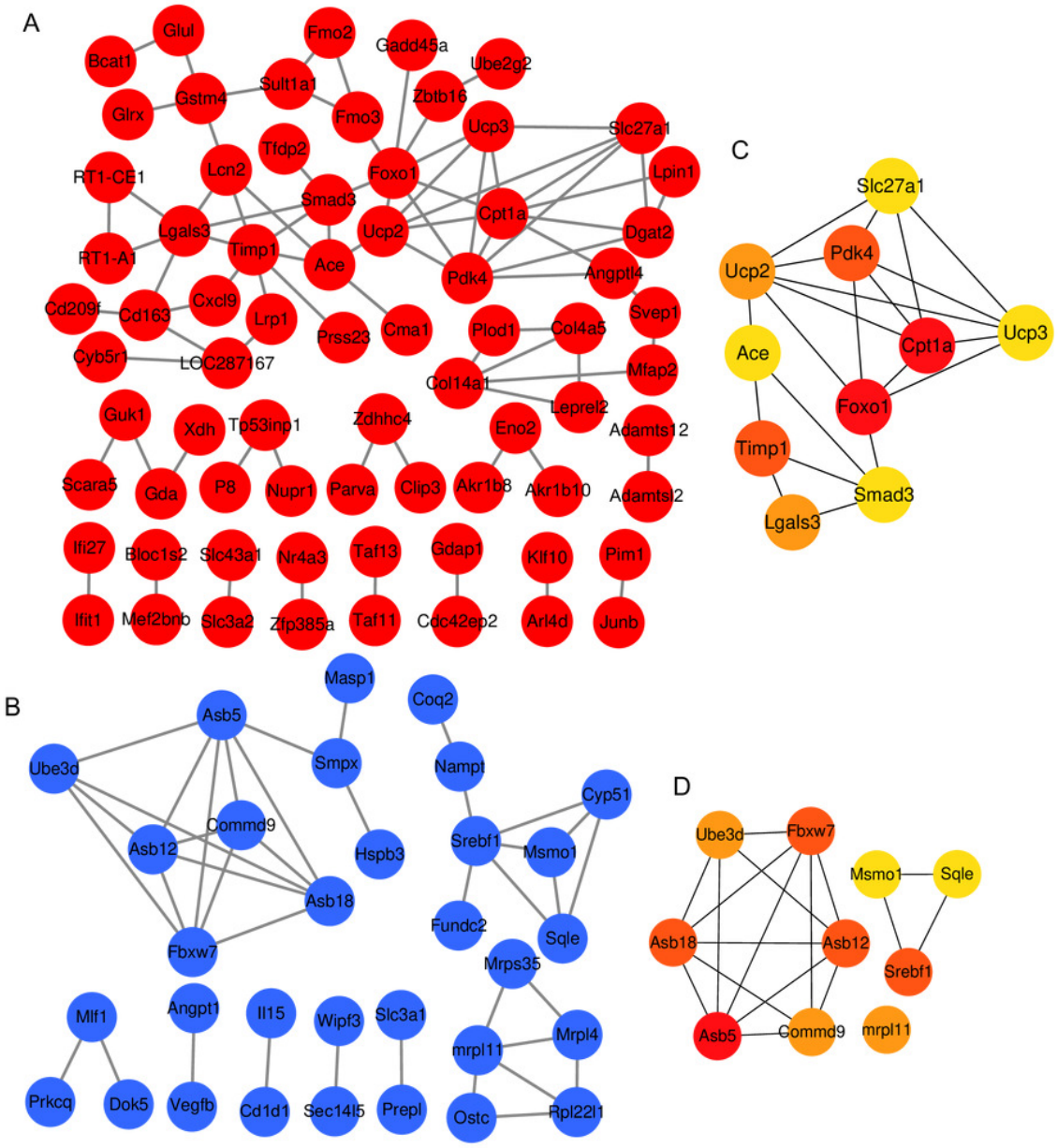
A
Glul
Fmo2
Gadd45a
Ube2g2
Bcat1
Sult1a1
Zbtb16
Gstm4
Glrx
Fmo3
Ucp3
Slc27a1
Tfdp2
Lcn2
Foxo1
Lpin1
RT1-CE1
Smad3
Cpt1a
Lgals3
Ucp2
Dgat2
Timp1
RT1-A1
Ace
Pdk4
Angptl4
Cd209f
Cd163
Cxcl9
Lrp1
Svep1
Prss23
Cma1
Plod1
Col4a5
Cyb5r1
LOC287167
Mfap2
Col14a1
Leprel2
Guk1
Xdh
Tp53inp1
Zdhhc4
Eno2
Adamts12
Scara5
Gda
P8
Nupr1
Parva
Clip3
Akr1b8
Akr1b10
Adamtsl2
Ifi27
Bloc1s2
Slc43a1
Nr4a3
Taf13
Gdap1
Klf10
Pim1
Ifit1
Mef2bnb
Slc3a2
Zfp385a
Taf11
Cdc42ep2
Arl4d
Junb
B
Masp1
Asb5
Coq2
Ube3d
Smpx
Nampt
Cyp51
Commd9
Asb12
Srebf1
Msmo1
Hspb3
Asb18
Fundc2
Sqle
Fbxw7
Mrps35
Mlf1
Angpt1
Il15
Wipf3
Slc3a1
mrpl11
Mrpl4
Prkcq
Dok5
Vegfb
Cd1d1
Sec14l5
Prepl
Ostc
Rpl22l1
C
Slc27a1
Ucp2
Pdk4
Ucp3
Ace
Cpt1a
Foxo1
Timp1
Smad3
Lgals3
D
Ube3d
Fbxw7
Msmo1
Sqle
Asb18
Asb12
Srebf1
Asb5
Commd9
mrpl11

Figure 4

Figure 4 The co-expressed lncRNAs-mRNAs pairs with high correlation coefficients.

(A) The biological process of dysregulated mRNAs in co-expressed lncRNAs-mRNAs pairs with high correlation coefficients. The GO terms of biological process were as follows : GO: 0055114 oxidation-reduction process; GO: 0009267 cellular response to starvation; GO: 0050776 regulation of immune response; GO: 0017144 drug metabolic process; GO: 0048701 embryonic cranial skeleton morphogenesis; GO: 0034097 response to cytokine; GO: 0006955 immune response; GO: 0046320 regulation of fatty acid oxidation; GO: 0030091 protein repair; GO: 0006749 glutathione metabolic process; GO: 0007568 aging; GO: 0043434 response to peptide hormone; GO 0008286 insulin receptor signaling pathway; GO: 0006739 NADP metabolic process; GO 0006355 regulation of transcription, DNA-templated; GO 0032870 cellular response to hormone stimulus. (B) The network of key genes and their co-expressed lncRNAs. The red represents upregulated gene in GK rats compared with aged-matched Wistar rats at the age of 3 and 4 weeks. The blue represents downregulated gene in GK rats compared with aged-matched Wistar rats at the age of 3 and 4 weeks. The diamond represents lncRNA, while the circle represents mRNA. The line between lncRNA and mRNA represents the co-expression coefficient. The range of correlation coefficients was from 0.9 to 0.993573997. (C). The relative expression of *Ephx2*, *Pdk4* and *Stc2*. (D) The relative expression of NONRATG017315.2, NONRATG010201.2, NONRATG011747.2, and NONRATG003318.2. Values are means ± SD, $*P < 0.05$, $**P < 0.01$, $***P < 0.001$ vs age-matched Wistar group, n = 6.

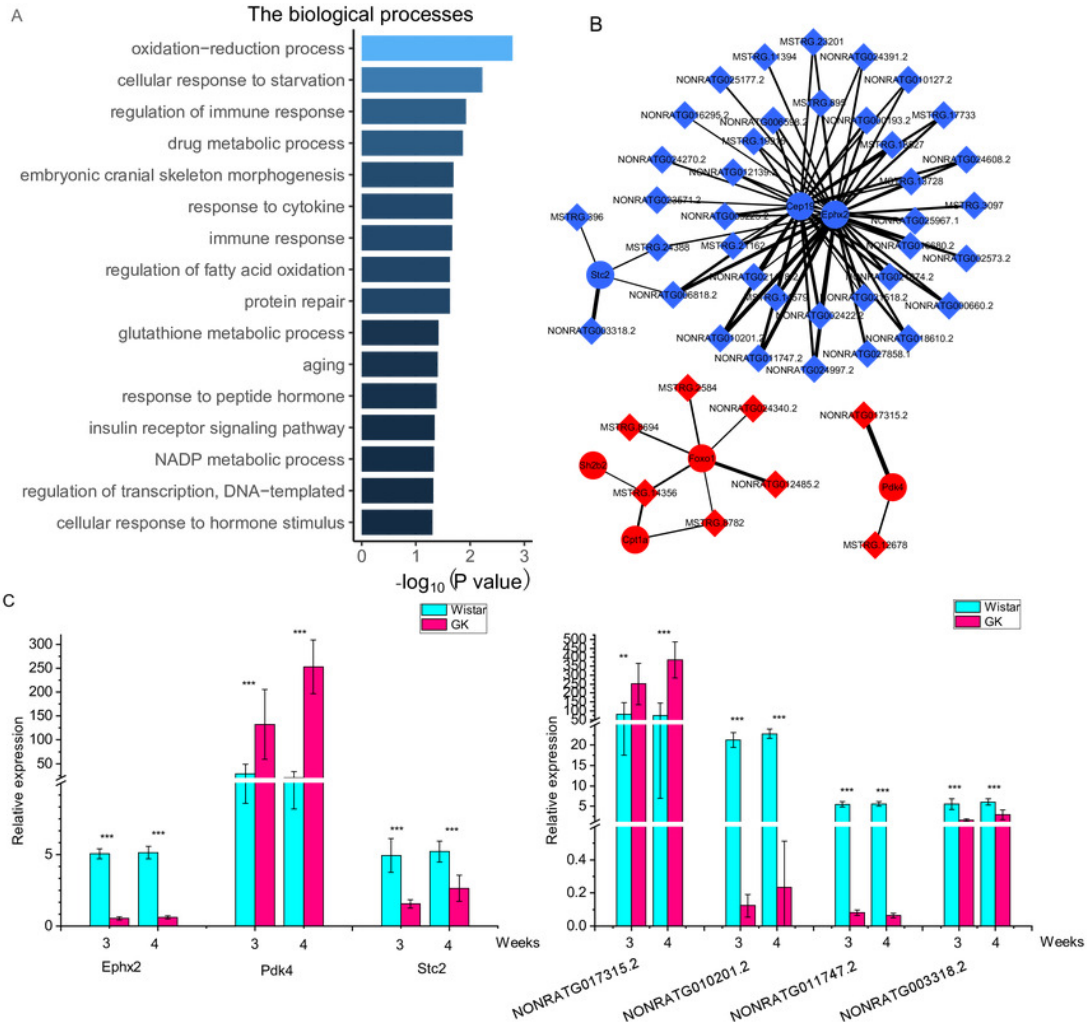
A
The biological processes
oxidation−reduction process
cellular response to starvation
regulation of immune response
drug metabolic process
embryonic cranial skeleton morphogenesis
response to cytokine
immune response
regulation of fatty acid oxidation
protein repair
glutathione metabolic process
aging
response to peptide hormone
insulin receptor signaling pathway
NADP metabolic process
regulation of transcription, DNA−templated
cellular response to hormone stimulus
0 1 2 3
-log10 (P value)
B
Stc2
Ephx2
Foxo1
Pdk4
Cpt1b
C
Wistar
GK
Relative expression
Weeks
Ephx2
Pdk4
Stc2
NONRATG017315.2
NONRATG010201.2
NONRATG011747.2
NONRATG003318.2

Figure 5

Figure 5 The differentially expressed target mRNAs for differentially expressed lncRNAs.

(A) Venn diagram of lncRNA-target mRNAs at 3 and 4 weeks. The DELs_target DEGs represents the target differentially expressed mRNAs of differentially expressed lncRNAs. (B) The network of overlapping lncRNA-target mRNAs at 3 and 4 weeks. The blue represents downregulated expression in GK rats compared with aged-matched Wistar rats at 3 and 4 weeks. The diamond represents lncRNA, the circle represents mRNA. (C) The relative expression of NONRATG011882.2-*Il15*, NONRATG013497.2-*Fbxw7*, and MSTRG.1662-*Ucp3*. Values are means ± SD, $*P < 0.05$, $**P < 0.01$, $***P < 0.001$ vs age-matched Wistar group, n=6. The red represents upregulated expression in GK rats compared with aged-matched Wistar rats at the age of 3 and 4 weeks.

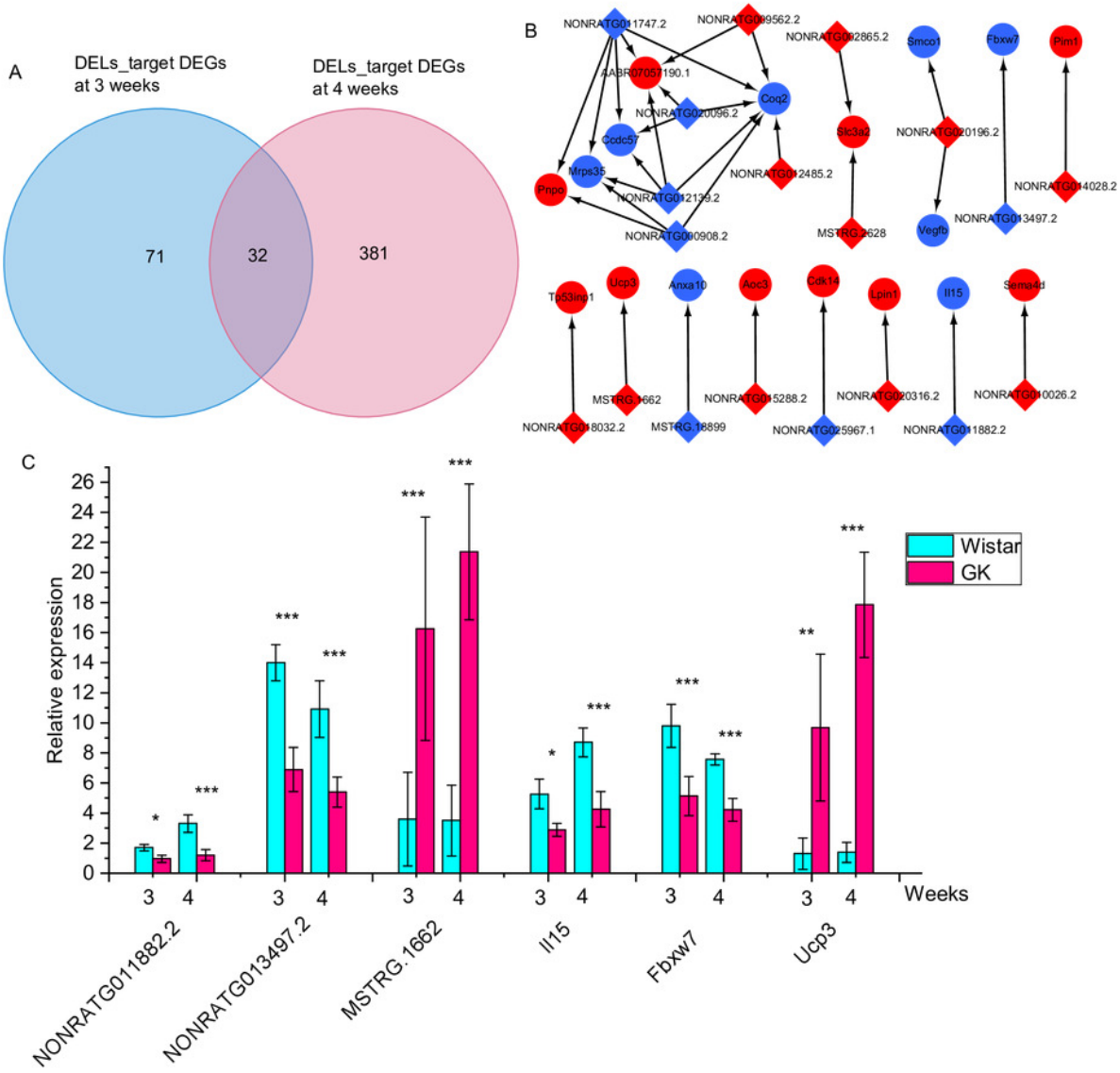
A
DELs_target DEGs at 3 weeks
DELs_target DEGs at 4 weeks
71
32
381
B
NONRATG011747.2
NONRATG009562.2
NONRATG002865.2
AABR07053190.1
Coq2
NONRATG020096.2
Ccdc57
Slc3a2
Mrps35
NONRATG012485.2
Pnpo
NONRATG012139.2
NONRATG000908.2
MSTRG.2628
Smco1
Fbxw7
Pim1
NONRATG020196.2
NONRATG014028.2
Vegfb
NONRATG013497.2
Tp53inp1
Ucp3
Anxa10
Aoc3
Cdk14
Lpin1
Il15
Sema4d
MSTRG.1662
NONRATG015288.2
NONRATG020316.2
NONRATG010026.2
NONRATG018032.2
MSTRG.18899
NONRATG025967.1
NONRATG011882.2
C
Relative expression
Wistar
GK
Weeks
NONRATG011882.2
NONRATG013497.2
MSTRG.1662
Il15
Fbxw7
Ucp3

Figure 6

Figure 6 The target miRNAs of DEGs and DELs in key lncRNA-mRNA pairs.

The light orange represents lncRNA. The light blue represents miRNA. The light green represents mRNA.

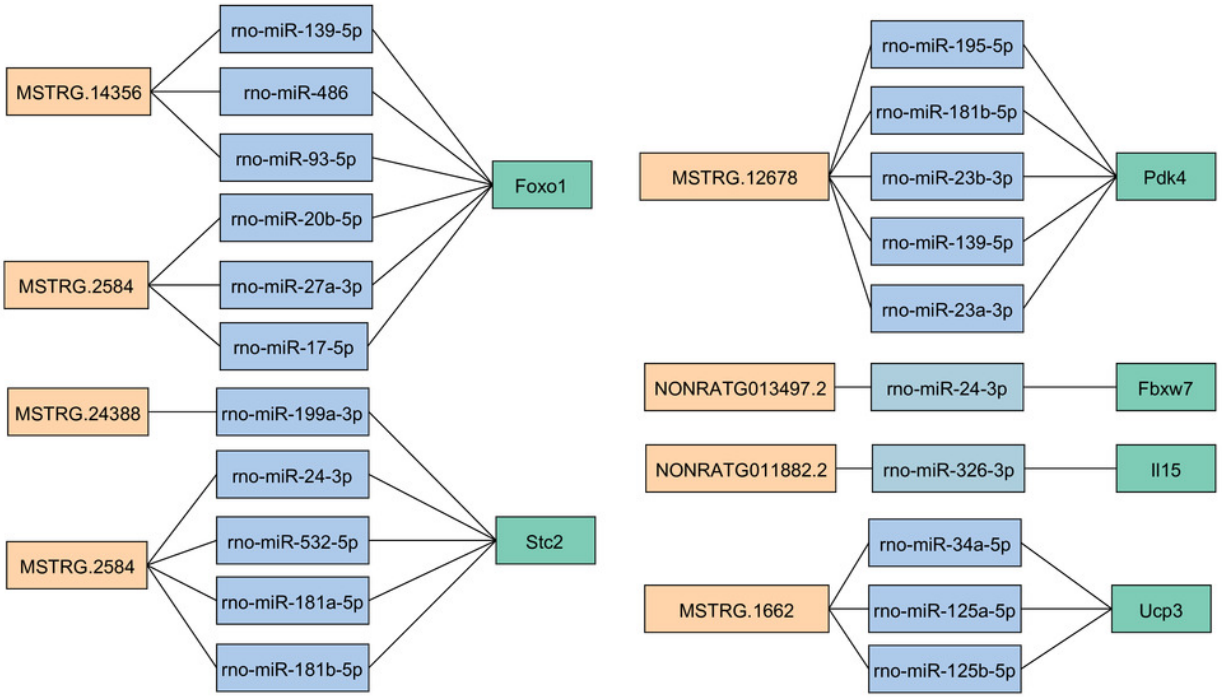

Table 1(on next page)

Table 1 The characteristics of rats.

Values are means ± SD, ***$P < 0.001$ vs age-matched Wistar group, n = 10.

1 Table 1 The characteristics of rats

Rats	Age, weeks	Plasma glucose, mmol/L	Plasma insulin, pmol/L	Weight, g
Wistar	3	5.05±0.39	157.66±64.52	88.92±7.08
	4	6.65±0.49	168.97±36.37	139.42±9.62
GK	3	7.82±0.43 ***	197.83±57.69	85.03±14.36
	4	11.13±0.29 ***	147.16±59.92	131.94±16.56

2 Values are means ± SD, ***$P < 0.001$ vs age-matched Wistar group, n = 10. SD: standard deviation.

Table 2(on next page)

Table 2 Top 10 nodes ranked by the degree in co-expressed lncRNA-mRNA network.

Table 2 Top 10 nodes ranked by the degree in co-expressed lncRNA-mRNA network.

ID (Name)	Type	Degree
ENSRNOG00000017286 (*Ephx2*)	mRNA	34
ENSRNOG00000005177 (*Tp53i3*)	mRNA	33
ENSRNOG00000026493 (*Cdnf*)	mRNA	32
MSTRG.2584	lncRNA	31
ENSRNOG00000024924 (*Cep19*)	mRNA	31
ENSRNOG00000000473 (*Pfdn6*)	mRNA	30
MSTRG.8694	lncRNA	28
MSTRG.14356	lncRNA	26
ENSRNOG00000010802 (*Ube3d*)	mRNA	25
ENSRNOG00000016937 (*Mtfr1l*)	mRNA	25